Supporting Information

Trichonas et al. 10.1073/pnas.1009179107

SI Materials and Methods

Surgical Induction of Retinal Detachment. Experimental retinal detachment was induced as previously described (1). Briefly, a 30-gauge needle was inserted into the subretinal space via an external transscleral transchoroidal approach, and 1% sodium hyaluronate (Provisc; Alcon) containing vehicle (0.05% DMSO and 0.8% cyclodextrin in PBS solution), Nec-1 (400 μM), and/or Z-VAD (300 μM; Alexis) was gently injected into the subretinal space to enlarge the retinal detachment.

Immunofluorescence. Immunofluorescence was performed as previously reported (2). The enucleated eyes were frozen in optimal cutting temperature compound (Sakura Finetechnical). Five-micrometer-thick sections were cut, air-dried, and fixed in cold acetone for 10 min. Rabbit anti-AIF (1:100; Cell Signaling Technology) and rat anti-CD11b (1:50; BD Biosciences) were used as primary antibodies and incubated at 4 °C overnight. A nonimmune serum was used as a negative control. Alexa Fluor 488-conjugated goat anti-rabbit IgG and Alexa Fluor 594-conjugated goat anti-rat IgG (Invitrogen) were used as secondary antibodies and incubated at room temperature for 1 h. The specimens were imaged by confocal microscopy using a Leica HCX APOL 40× lens.

In Situ Hybridization. Partial sequence of mouse RIP3 gene was amplified by RT-PCR using AGCACAGGACACATCAGTTGG and CTTGAGGCAGTAGTTCTTGGTG, and cloned into the pCR-II vector (Invitrogen). Digoxigenin-labeled riboprobe was hybridized at 61 °C overnight, followed by stringent washes. The cryosections were then treated with an alkaline phosphatase-conjugated antidigoxigenin antibody (Roche). Hybridization signals were visualized with BM purple AP substrate (Roche).

TEM. TEM was performed as previously described (1). More than 200 photoreceptors per eye were photographed and subjected to quantification of cell death modes in a masked fashion. Photoreceptors showing cellular shrinkage and nuclear condensation were defined as apoptotic cells, whereas photoreceptors associated with cellular and organelle swelling and discontinuities in plasma and nuclear membrane were defined as necrotic cells. Electron-dense granular materials were labeled simply as end-stage cell death/unclassified, because these materials are reported to occur subsequent to both apoptotic and necrotic cell death (3, 4).

RNA Extraction, RT-PCR, and Quantitative Real-Time PCR. Total RNA extraction and reverse transcription were performed as previously reported (1, 5). A real-time PCR assay was performed with the Prism 7700 Sequence Detection System (Applied Biosystems). TaqMan gene expression assays were used to check the expression of RIP1 (Rn01757378_m1), RIP3 (Rn00595154_m1), and TNF-α (Rn99999017_m1). For relative comparison of each gene, we analyzed the Ct value of real-time PCR data with the ΔΔCt method normalizing by an endogenous control (18S ribosomal RNA).

ELISA. The protein contents in retinal extract were determined with ELISA kits for protein carbonyls (Cell Biolabs), MCP-1 [rat MCP-1 (Thermo Scientific), mouse MCP-1 (R&D Systems)], and TNF-α [rat TNF-α (Invitrogen), mouse TNF-α (R&D Systems)] according to manufacturer instructions.

Western Blotting. The vitreous and neural retina, combined, was collected on day 3 after retinal detachment. Samples were run on 4% to 12% SDS-polyacrylamide gel electrophoresis and transferred onto PVDF membrane. After blocking with 3% nonfat dried milk, the membrane was reacted with RIP3 (1:10,000; Sigma), RIP1 (1:2,000; BD Biosciences), phosphoserine (1:2,000; Enzo), or anti-phosphorylated NF-κB p65 (1:1,000; Cell Signaling Technology) antibody. They were then developed with enhanced chemiluminescence. Lane-loading differences were normalized by β-tubulin (1:1,000; Cell Signaling Technology).

Immunoprecipitation. Equal amount of retinal lysates (1 mg) were incubated with 1 μg anti-RIP1 antibody (BD Biosciences) and 20 μL of protein A/G agarose beads (Thermo Scientific) at 4 °C overnight. Beads were washed five times with lysis buffer and Tris-buffered saline solution and the immunopellets were then subjected to Western blotting.

In Vivo PI Staining. Five microliters of PI (50 μg/mL) were injected into the subretinal space 3 d after retinal detachment. After 2 h, the eyes were enucleated and 10-μm-thick cryosections were cut, air-dried, and fixed in 100% ethanol. DAPI was used to counterstain the nuclei. The center of the detached retina was photographed with a fluorescence microscope, and the number of PI-positive cells in ONL was analyzed by ImageJ software.

Reagents. Goat anti-mouse/rat TNF-α blocking antibody was purchased from R&D Systems. The rat eyes were subretinally injected with 1% of sodium hyaluronate containing 0.1 mg/mL of anti–TNF-α antibody or control goat antibody. Nec-4 and PCI (IDN6556) were prepared as described in refs. 6 and 7, respectively.

1. Hisatomi T, et al. (2008) HIV protease inhibitors provide neuroprotection through inhibition of mitochondrial apoptosis in mice. *J Clin Invest* 118:2025–2038.
2. Murakami Y, et al. (2008) Inhibition of nuclear translocation of apoptosis-inducing factor is an essential mechanism of the neuroprotective activity of pigment epithelium-derived factor in a rat model of retinal degeneration. *Am J Pathol* 173:1326–1338.
3. Hisatomi T, et al. (2003) Clearance of apoptotic photoreceptors: elimination of apoptotic debris into the subretinal space and macrophage-mediated phagocytosis via phosphatidylserine receptor and integrin alphavbeta3. *Am J Pathol* 162:1869–1879.
4. Erickson PA, Fisher SK, Anderson DH, Stern WH, Borgula GA (1983) Retinal detachment in the cat: The outer nuclear and outer plexiform layers. *Invest Ophthalmol Vis Sci* 24:927–942.
5. Nakazawa T, et al. (2006) Characterization of cytokine responses to retinal detachment in rats. *Mol Vis* 12:867–878.
6. Teng X, et al. (2007) Structure-activity relationship study of [1,2,3]thiadiazole necroptosis inhibitors. *Bioorg Med Chem Lett* 17:6836–6840.
7. Hoglen NC, et al. (2004) Characterization of IDN-6556 (3-[2-(2-tert-butyl-phenylaminooxalyl)-amino]-propionylamino]-4-oxo-5-(2,3,5,6-tetrafluoro-phenoxy)-pentanoic acid): A liver-targeted caspase inhibitor. *J Pharmacol Exp Ther* 309: 634–640.

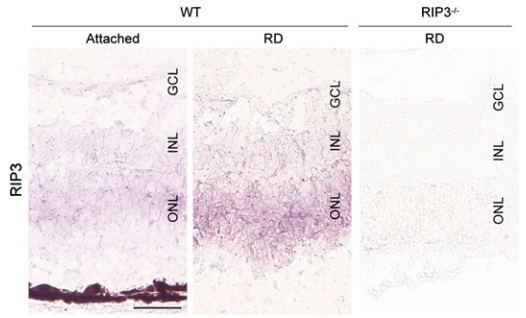

Fig. S1. In situ hybridization analysis of RIP3. RIP3 signal was detected in retinal tissue, especially in the ONL, after retinal detachment. The retina from *Rip3*$^{-/-}$ animals was used as negative control. GCL, ganglion cell layer; INL, inner nuclear layer. (Scale bar, 50 μm.)

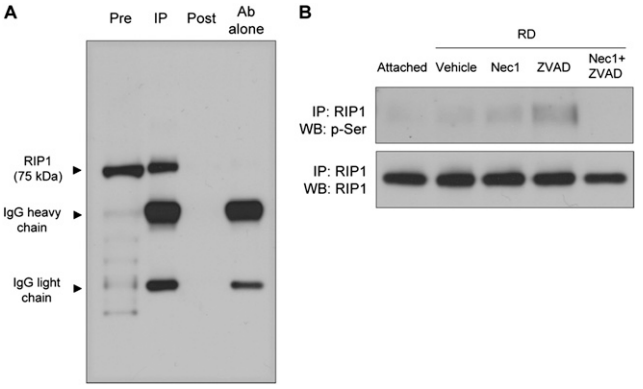

Fig. S2. (*A*) Immunoprecipitation of RIP1 from retinal lysates. One milligram of retinal lysates was incubated with anti-RIP1 antibody and protein A/G agarose beads. Extracts before (Pre) and after (Post) immunoprecipitation and the immunopellets (IP) were run on a 4% to 12% SDS/PAGE and blotted with anti-RIP1 antibody. Anti-RIP1 antibody alone was used as negative control. Extracts after immunoprecipitation showed almost complete immunodepletion of RIP1 from the retinal extract. (*B*) Phosphorylation of RIP1 after retinal detachment. RIP was immunoprecipitated from lysates of untreated retina and of retina 2 d after retinal detachment with treatment of vehicle, Nec-1, Z-VAD, or Nec-1 plus Z-VAD, and then assessed for phosphorylation by Western blotting. RIP1 phosphorylation was elevated especially in Z-VAD-treated detached retina, and this phosphorylation was inhibited by Nec-1 plus Z-VAD.

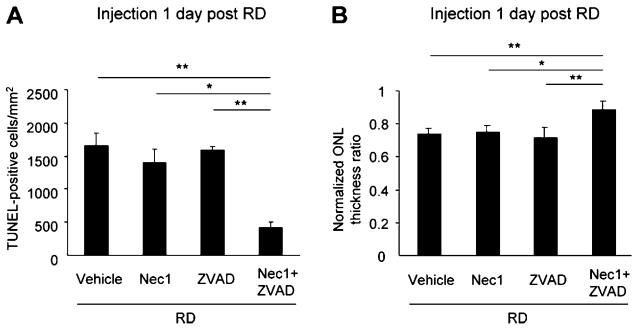

Fig. S3. Quantification of TUNEL-positive photoreceptors (*A*) and ONL thickness ratio (*B*) on day 3 after retinal detachment in rats ($n = 4–5$). Five microliters of Nec-1 (2 mM) and/or Z-VAD (3 mM) were injected intravitreally 1 d after retinal detachment induction. Treatment with Nec-1 plus Z-VAD significantly decreased the number of TUNEL-positive cells and prevented the reduction of ONL thickness ratio after retinal detachment (*$P < 0.05$; **$P < 0.01$).

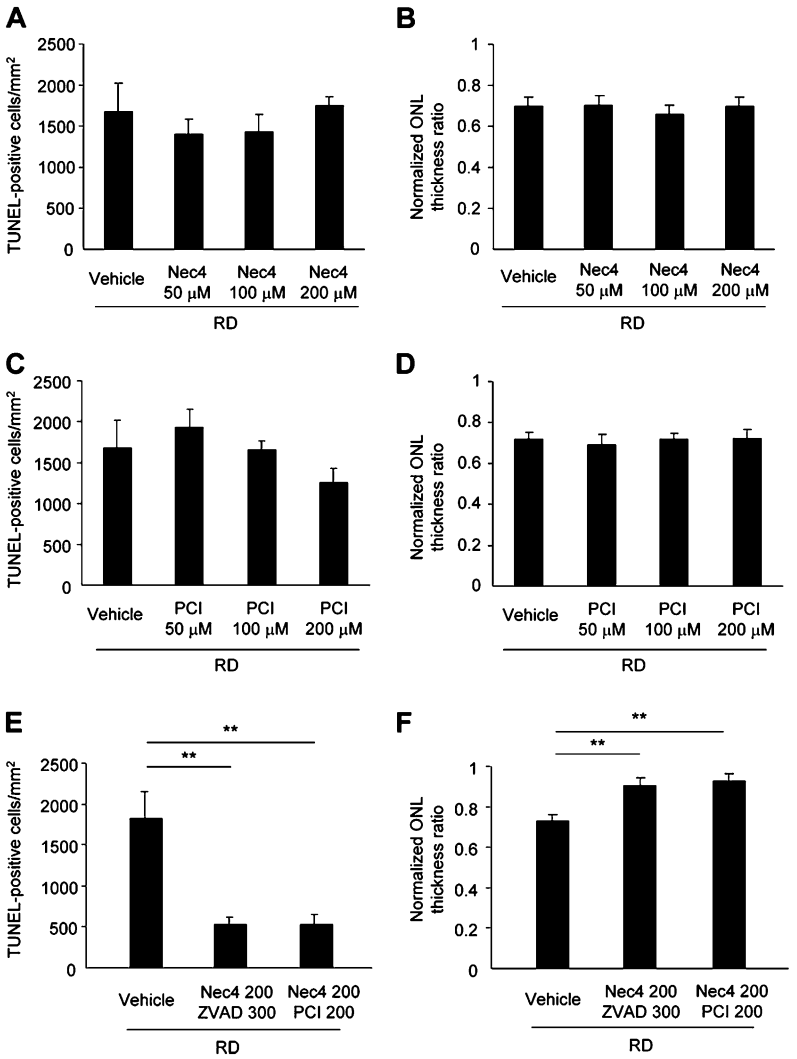

Fig. S4. Quantification of TUNEL-positive photoreceptors (*A*, *C*, and *E*) and ONL thickness ratio (*B*, *D*, and *F*) on day 3 after retinal detachment in rats ($n = 5–6$). Nec-4, PCI, and/or Z-VAD were injected subretinally at the indicated doses. Treatment with Nec4 or PCI alone did not show any protective effect (*A–D*). In contrast, Nec-4 plus Z-VAD or Nec-4 plus PCI treatment significantly suppressed photoreceptor loss after retinal detachment (*E* and *F*). $^{**}P < 0.01$.

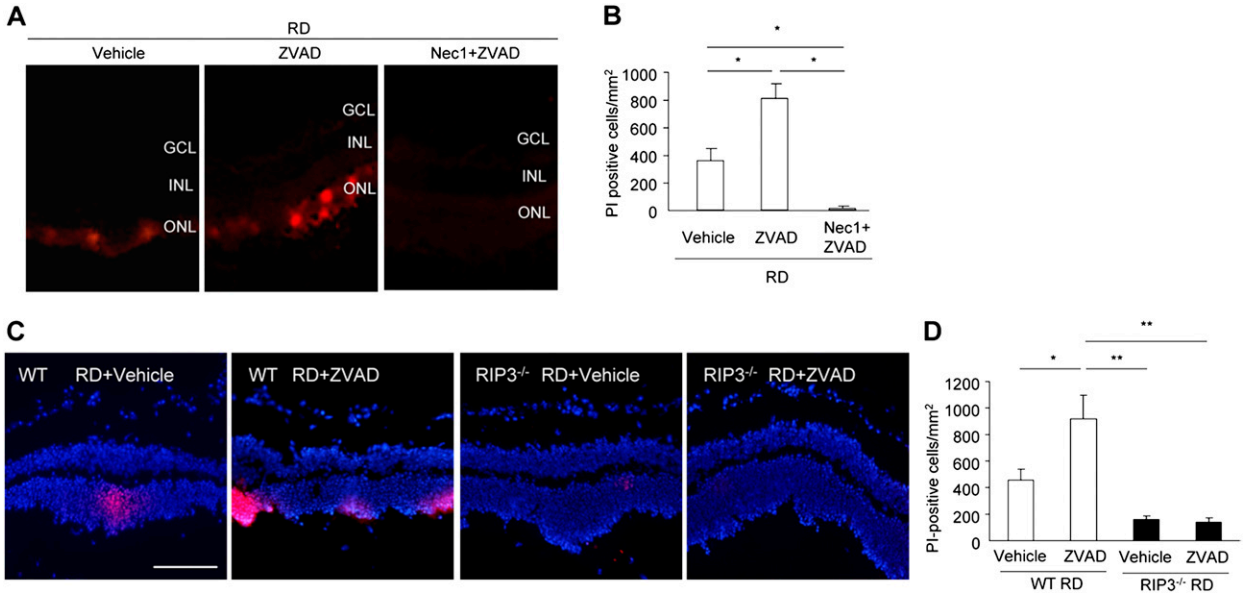

Fig. S5. PI staining (*A* and *C*) and quantification of PI-positive photoreceptors (*B* and *D*) on day 3 after retinal detachment in retina treated with vehicle, Z-VAD, or Nec-1 plus Z-VAD (n = 6 each; *A* and *B*) and in WT and *Rip3*$^{-/-}$ retina (n = 5–6; *C* and *D*); *$P < 0.05$; **$P < 0.01$. (Scale bar, 100 μm.)

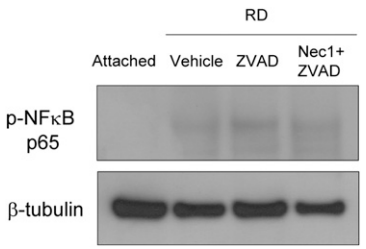

Fig. S6. Western blot analysis for phospho-NFκB p65 in control retina without retinal detachment and in retina 3 d after retinal detachment with treatment of vehicle, Z-VAD, or Nec-1 plus Z-VAD. Lane-loading differences were normalized by the level of β-tubulin.

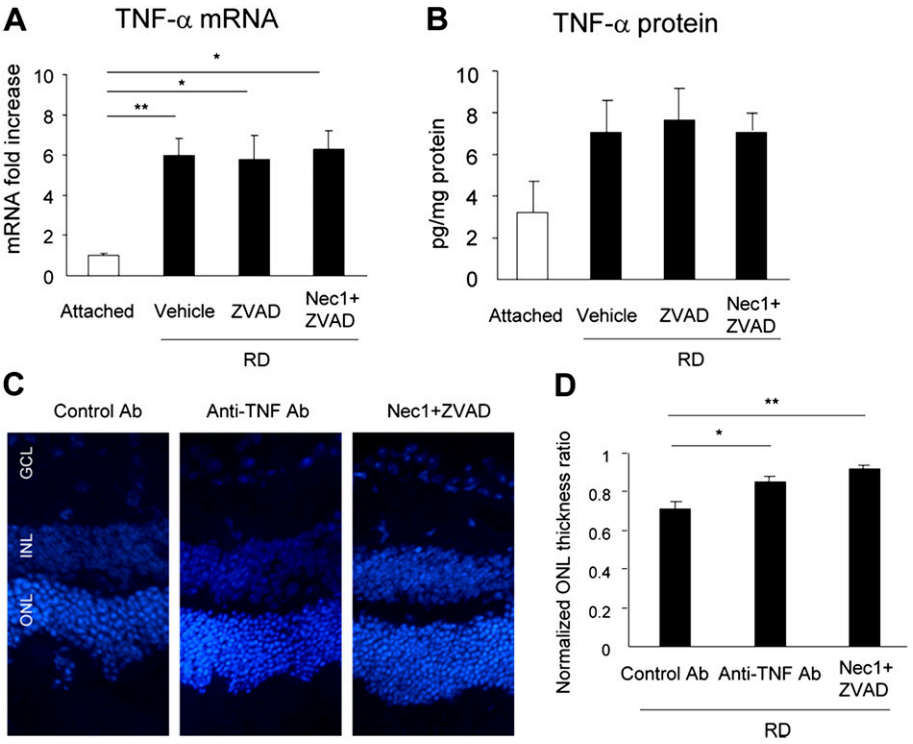

Fig. S7. (*A*) Quantitative real-time PCR analysis for TNF-α in control retina without retinal detachment ($n = 9$) and in retina 3 d after retinal detachment with treatment of vehicle ($n = 9$), Z-VAD ($n = 8$), or Nec-1 plus Z-VAD ($n = 9$). (*B*) ELISA for TNF-α in retina without retinal detachment ($n = 5$) and in retina 3 d after retinal detachment with treatment of vehicle ($n = 5$), Z-VAD ($n = 5$), or Nec-1 plus Z-VAD ($n = 6$). DAPI staining (*C*) and quantification of ONL thickness ratio (*D*) in detached retina treated with anti–TNF-α antibody, control antibody, or ZVAD plus Nec-1 on day 3 after retinal detachment ($n = 4$ each); $^*P < 0.05$; $^{**}P < 0.01$.

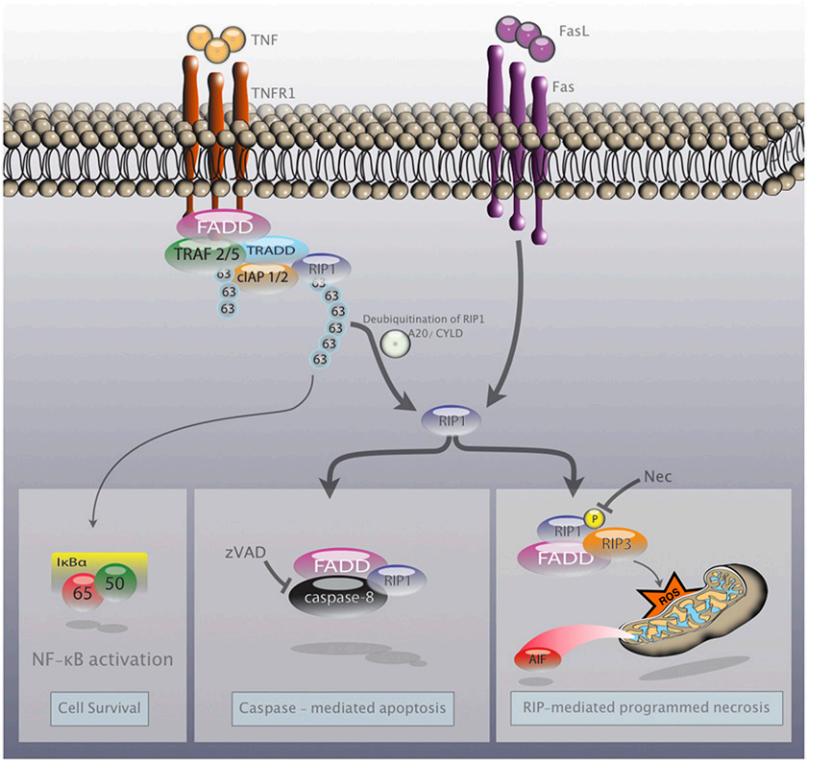

Fig. S8. Schematic of RIP signaling pathway. RIP1 mediates prosurvival NF-κB activation through polyubiquitination of RIP1 in response to TNF-α. When RIP1 is unubiquitinated, RIP1 switches function to a regulator of cell death. RIP1 forms a death signaling complex with Fas-associated death domain (FADD) and caspase-8 after stimulation of death domain receptors, and induces caspase-dependent apoptosis. In conditions in which caspase pathway is blocked, RIP1 kinase is activated in RIP1–RIP3 complex and promotes programmed necrosis. TRAF2, tumor necrosis factor-receptor associated signaling adaptor; TRADD, TNF receptor-associated death domain; cIAP, cellular inhibitor of apoptosis; CYLD, cylindromatosis.